

## Supporting Information

### **A carbazole-functionalized metal–organic framework for efficient detection of antibiotics, pesticides and nitroaromatic compounds**

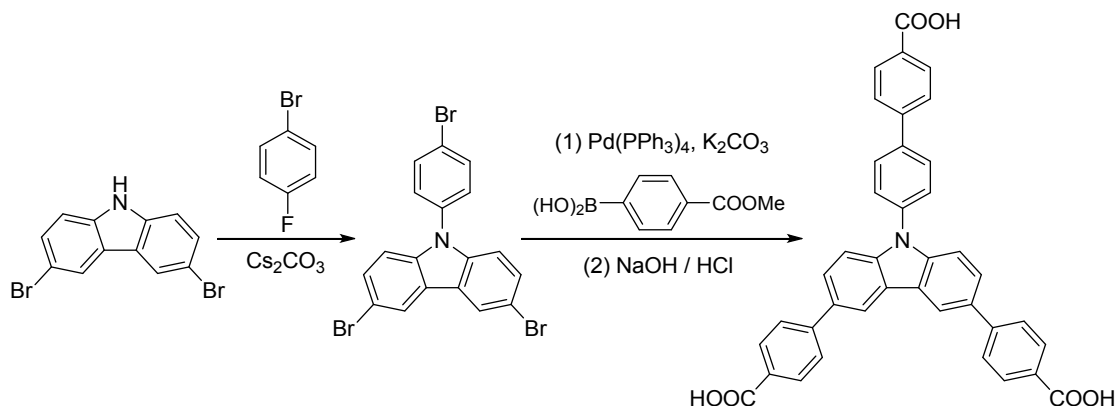
*Ning Xu, Qinghua Zhang, and Guoan Zhang\**

Key Laboratory of Material Chemistry for Energy Conversion and Storage, Ministry of Education,  
Hubei Key Laboratory of Materials Chemistry and Service Failure, School of Chemistry and  
Chemical Engineering, Huazhong University of Science and Technology, Wuhan 430074, P.R. China  
E-mail: [zhangguoan@gmail.com](mailto:zhangguoan@gmail.com) (G. A. Zhang), Tel.: +86-27-87559068; Fax: +86-27-87543632

## Contents

Section 1. Synthesis of H <sub>3</sub> CBCD.....	S3
Section 2. General characterizations and structural information.....	S7
Section 3. Detection of antibiotics.....	S11
Section 4. Detection of NACs and pesticides.....	S15
References.....	S18

## Section 1. Synthesis of H<sub>3</sub>CBCD



**Scheme S1.** The synthetic route for the H<sub>3</sub>CBCD ligand.

### (a) Synthesis of 3,6-dibromo-9-(4-bromophenyl)-9H-carbazole

3,6-dibromo-9H-carbazole (0.65 g, 2.0 mmol), 1-bromo-4-fluorobenzene (0.88 mL, 8.0 mmol), cesium carbonate (2.61 g, 8.0 mmol) and DMF (15 mL) were mixed in a 50 mL round bottom flask. The mixture was stirred at 150 °C under air atmosphere for 24 h and then cooled to room temperature. Dichloromethane (50 mL) and H<sub>2</sub>O (150 mL) were added, and the organic phase was separated. The aqueous phase was then extracted three times with dichloromethane (50 mL). The obtained organic phase was washed with saturated brine, dried over anhydrous MgSO<sub>4</sub>. After removing the organic solvent by rotary evaporation, the residue was purified by column chromatography with petroleum ether as eluent to obtain a light yellow solid product (0.68 g, 70.8% yield). <sup>1</sup>H NMR (400 MHz, CDCl<sub>3</sub>): δ (ppm)= 7.220 (d, 2H), 7.386 (d, 2H), 7.510 (d, 2H), 7.744 (d, 2H), 8.191 (s, 2H).

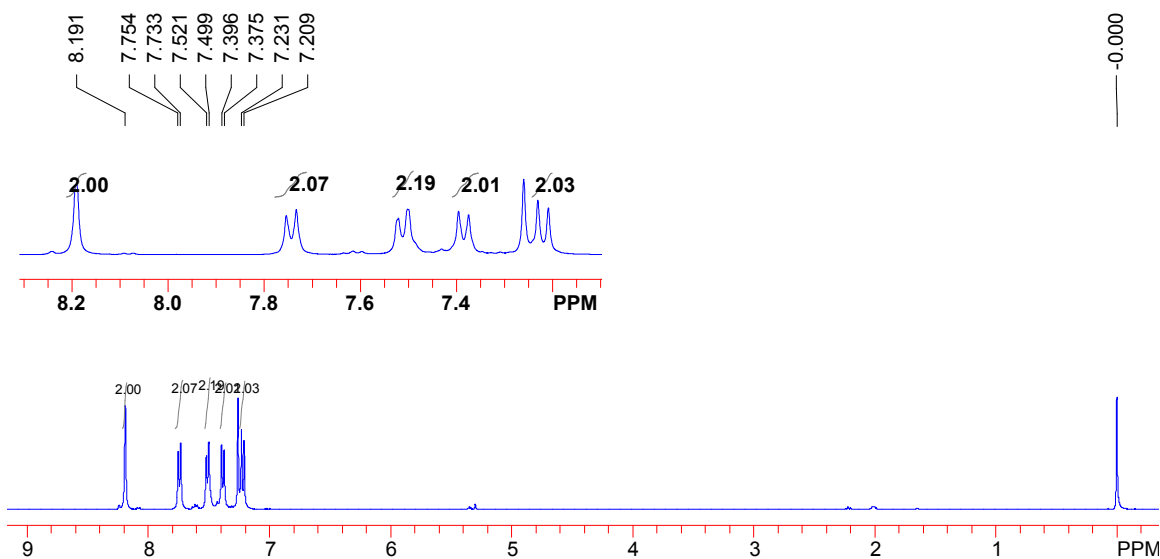


**Fig. S1.**  $^1\text{H-NMR}$  spectra of 3,6-dibromo-9-(4-bromophenyl)-9H-carbazole.

**(b) Synthesis of Dimethyl 4,4'-(9-(4'-(methoxycarbonyl)-[1,1'-biphenyl]-4-yl)-9H-carbazole-3,6-diyl)dibenzoate**

3,6-dibromo-9-(4-bromophenyl)-9H-carbazole (0.48 g, 1.0 mmol), methyl 4-boronobenzoate (0.72 g, 4.0 mmol),  $\text{Pd}(\text{PPh}_3)_4$  (0.12 g, 0.1 mmol) and  $\text{K}_2\text{CO}_3$  (1.11 g, 8.0 mmol) were mixed in a 100 mL Schlenk flask. After vacuumized and refilled with  $\text{N}_2$  for three times, toluene-methanol-water (20 ml, 10 ml, 10 ml) was added. The mixture was stirred at 80 °C for 24 h and then cooled to room temperature. After removing the organic phase under vacuum, dichloromethane (100 mL) and  $\text{H}_2\text{O}$  (50 mL) were added. The organic phase was separated and then the aqueous phase was extracted three times with dichloromethane (50 mL). The combined organic phases were washed with saturated brine, dried over anhydrous  $\text{MgSO}_4$ . After removing the organic solvent by rotary evaporation, the residue was purified by column chromatography with dichloromethane/ethyl acetate (30/1, v/v) as eluent to obtain a white solid product (0.45 g, 69.7% yield).  $^1\text{H NMR}$  (400 MHz,  $\text{CDCl}_3$ ):  $\delta$  (ppm)= 3.970 (d, 9H), 7.563 (d, 2H), 7.703-7.824 (m, 10H), 7.900 (d, 2H), 8.144-8.199 (m, 6H), 8.472 (s, 2H).

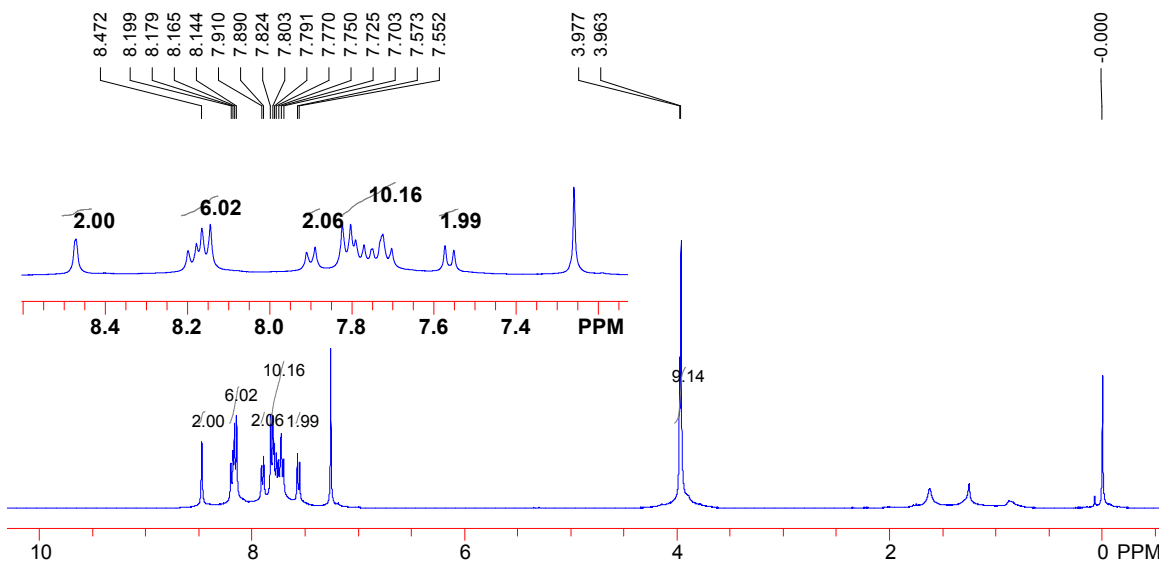


**Fig. S2.**  $^1\text{H-NMR}$  spectra of Dimethyl 4,4'-(9-(4'-(methoxycarbonyl)-[1,1'-biphenyl]-4-yl)-9H-carbazole-3,6-diyl)dibenzoate.

**(c) Synthesis of 4,4'-(9-(4'-carboxy-[1,1'-biphenyl]-4-yl)-9H-carbazole-3,6-diyl)dibenzoic acid**

0.45 g (0.70 mmol) of Dimethyl 4,4'-(9-(4'-(methoxycarbonyl)-[1,1'-biphenyl]-4-yl)-9H-carbazole-3,6-diyl)dibenzoate was dissolved in THF (30 mL), and then 35 mL 2 M NaOH aqueous solution was added. The solution was stirred at 65 °C for 12 h and the THF was removed in vacuum. Concentrated hydrochloric acid was added to the remaining aqueous solution until the solution became acidic (pH = 2~3). The solid was collected by filtration, washed several times with distilled water, and dried under vacuum to give a light yellow solid product (0.41 g, 97.5% yield). IR (KBr,  $\text{cm}^{-1}$ ): 2961 (w), 1687 (s), 1602 (s), 1525 (w), 1476 (m), 1413 (m), 1366 (m), 1272 (s), 1234 (s), 1181 (s), 1112 (w), 811 (m), 774 (s), 716 (w).  $^1\text{H NMR}$  (400 MHz,  $\text{DMSO-}d_6$ ):  $\delta$  (ppm)= 7.597 (d, 2H), 7.846 (d, 2H), 7.909 (d, 2H), 7.978 (t, 6H), 8.093 (t, 8H), 8.909 (s, 2H), 13.011 (s, 3H). ESI-MS calcd for  $\text{C}_{39}\text{H}_{24}\text{NO}_6[\text{M-H}]^-$ : 602.1604, found 602.1625.

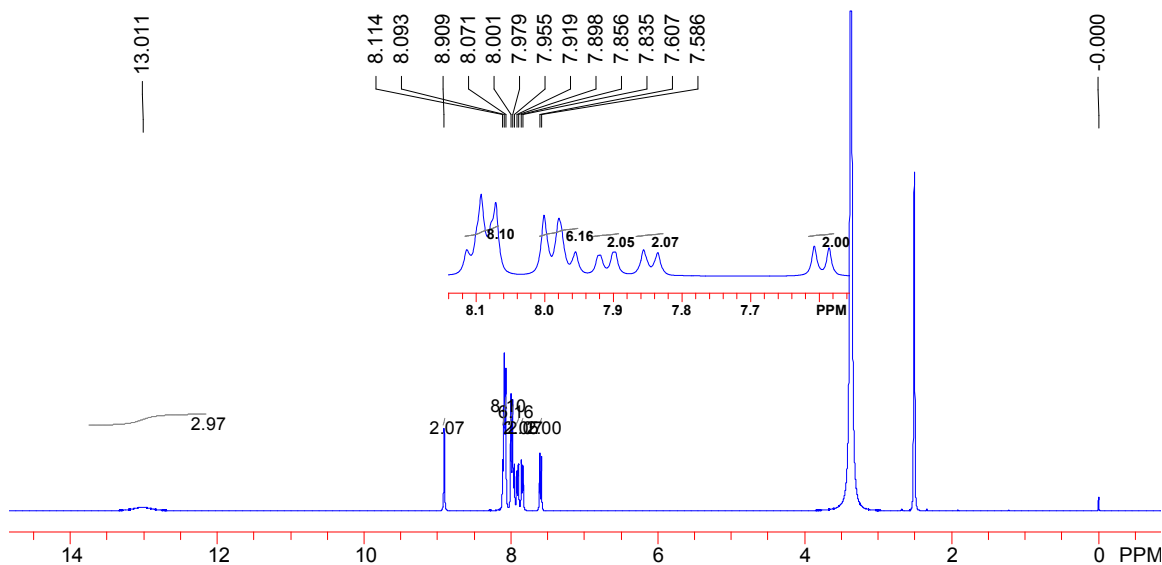


**Fig. S3.**  $^1\text{H-NMR}$  spectra of 4,4'-(9-(4'-carboxy-[1,1'-biphenyl]-4-yl)-9H-carbazole-3,6-diyl) dibenzoic acid.

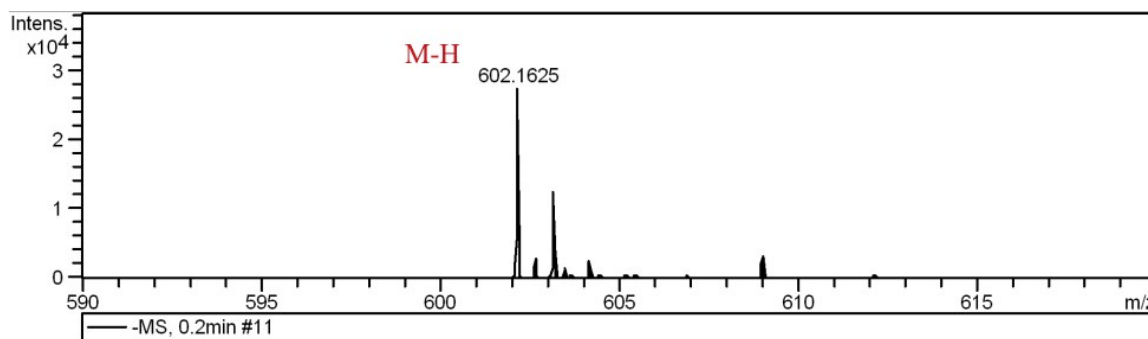


**Fig. S4.** Mass spectra of 4,4'-(9-(4'-carboxy-[1,1'-biphenyl]-4-yl)-9H-carbazole-3,6-diyl) dibenzoic acid.

## Section 2. General characterizations and structural information

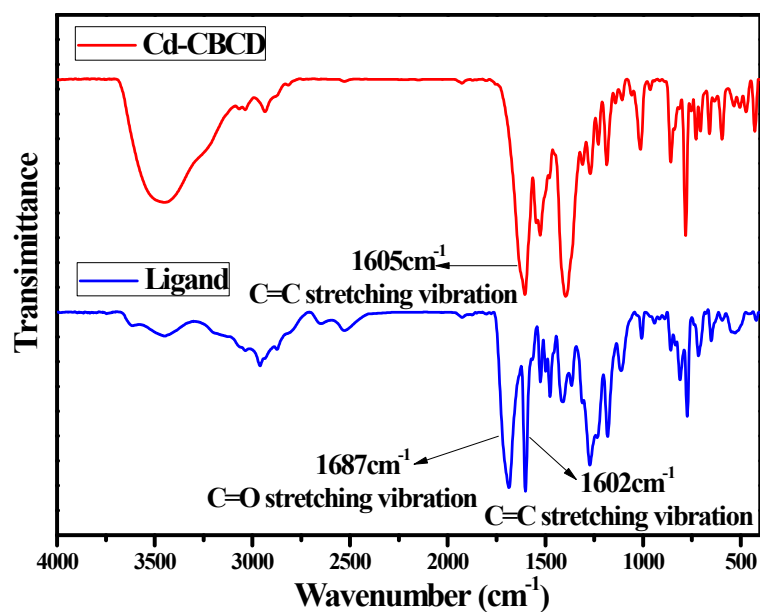


Fig. S5. IR spectra of the free ligand and Cd-CBCD.

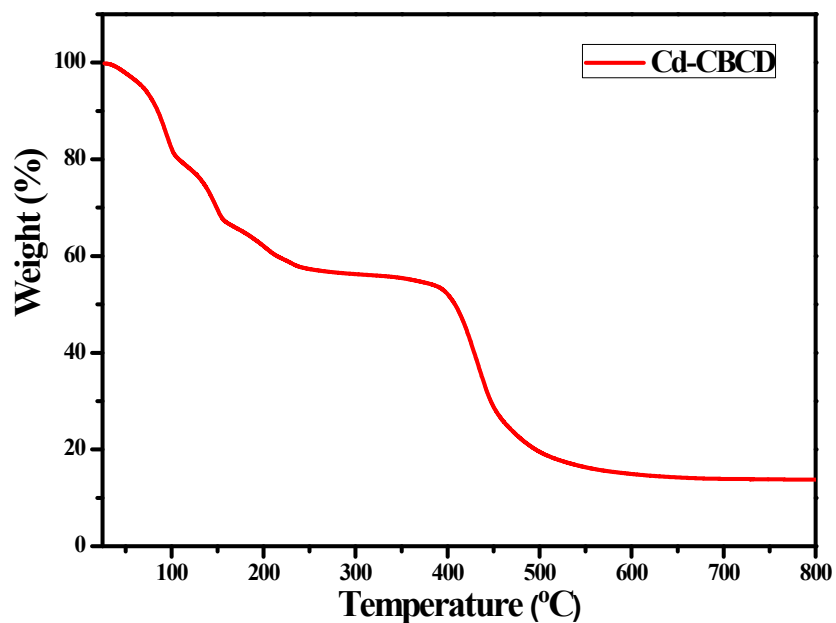


Fig. S6. TGA curve of Cd-CBCD.

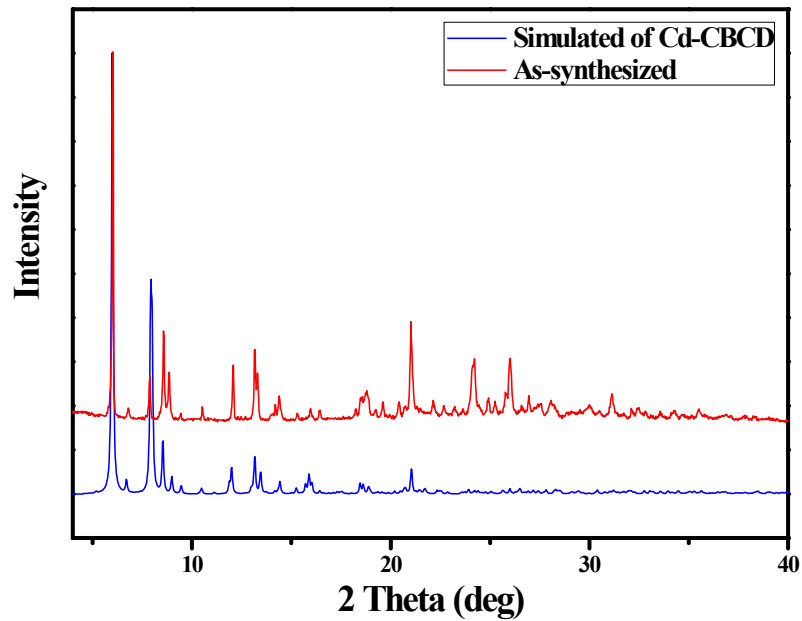


Fig. S7. XRD patterns of Cd-CBCD.

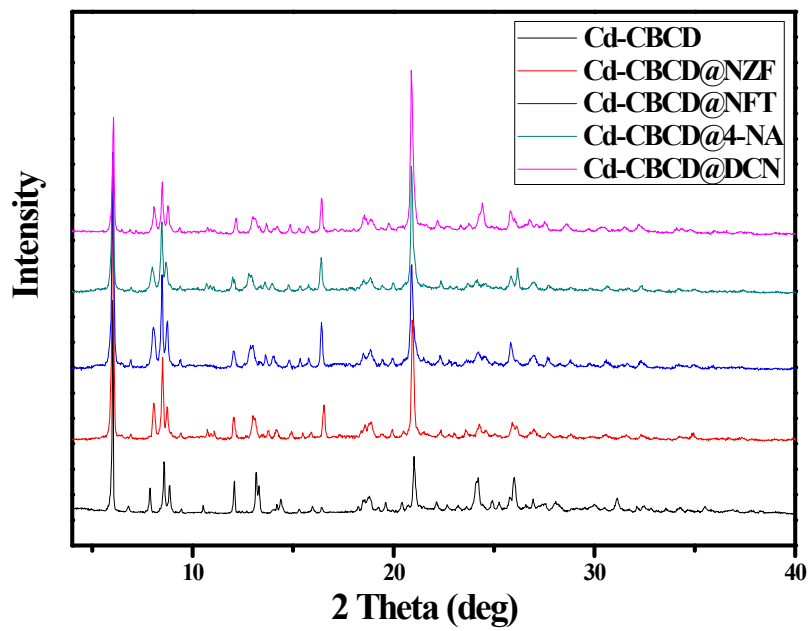


Fig. S8. PXRD patterns of Cd-CBCD after the detection of different analytes.



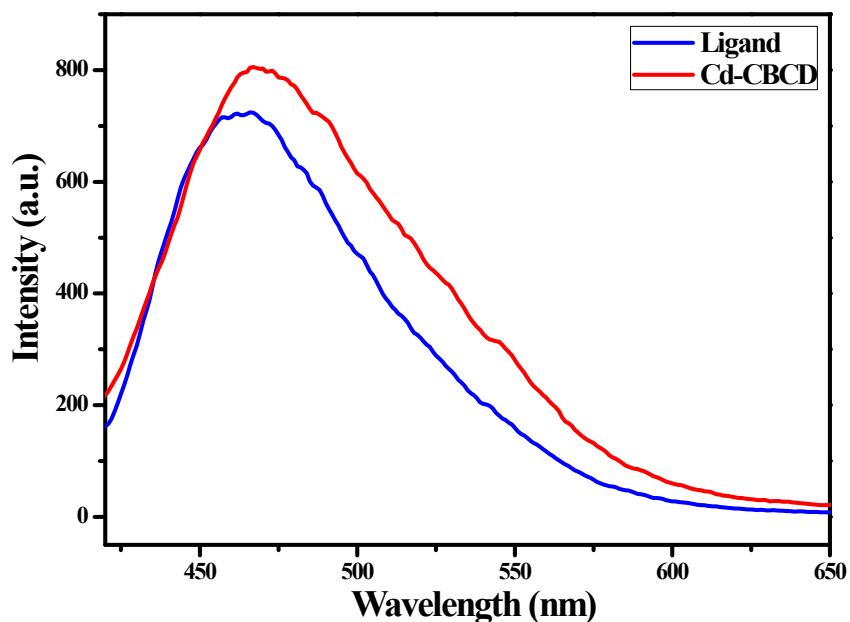


Fig. S9. Solid-state luminescence spectra of the free ligand and Cd-CBCD.

Table S1. Selected bond lengths (Å) and angles (deg) for Cd-CBCD.

<b>Cd-CBCD</b>			
Cd(1)-O(5) #1	2.207(2)	Cd(1)-O(5)#2	2.207(2)
Cd(1)-O(1)#3	2.294(2)	Cd(1)-O(1)	2.294(2)
Cd(1)-O(8)	2.355(2)	Cd(1)-O(8)#3	2.355(2)
Cd(2)-O(6)#2	2.213(2)	Cd(2)-O(7)	2.306(3)
Cd(2)-O(2)	2.311(2)	Cd(2)-O(3)#4	2.317(3)
Cd(2)-O(4)#4	2.376(3)	Cd(2)-O(1)	2.439(2)
Cd(2)-O(8)	2.553(3)		
O(5)#1-Cd(1)-O(5)#2	180.0	O(5)#1-Cd(1)-O(1)#3	91.29(9)
O(5)#2-Cd(1)-O(1)#3	88.71(9)	O(5)#1-Cd(1)-O(1)	88.71(9)
O(5)#2-Cd(1)-O(1)	91.29(9)	O(1)#3-Cd(1)-O(1)	180.0
O(5)#1-Cd(1)-O(8)	85.71(9)	O(5)#2-Cd(1)-O(8)	94.29(9)
O(1)#3-Cd(1)-O(8)	100.46(9)	O(1)-Cd(1)-O(8)	79.54(9)

---

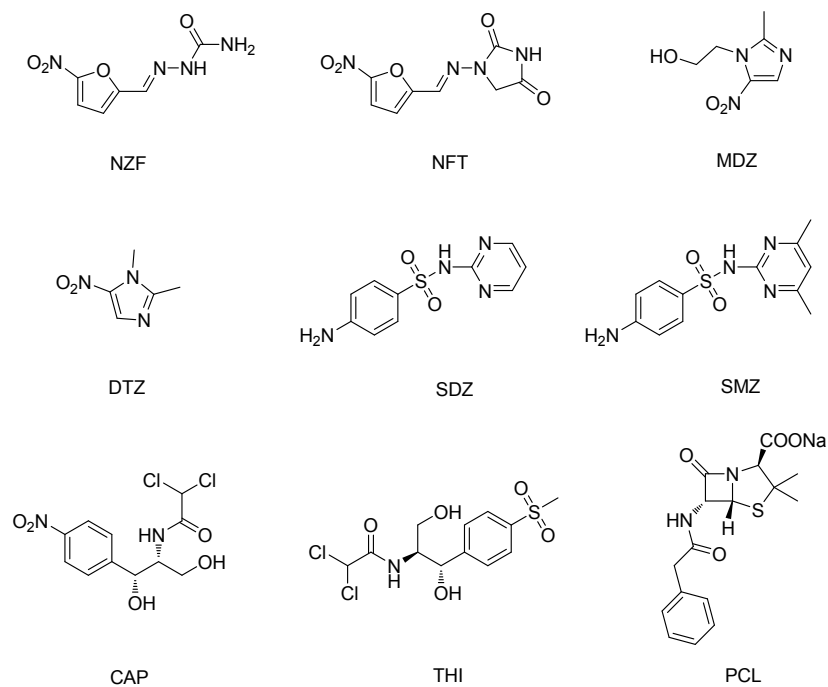
O(5)#1-Cd(1)-O(8)#3	94.29(9)	O(5)#2-Cd(1)-O(8)#3	85.71(9)
O(1)#3-Cd(1)-O(8)#3	79.54(9)	O(1)-Cd(1)-O(8)#3	100.46(9)
O(8)-Cd(1)-O(8)#3	180.0	O(6)#2-Cd(2)-O(7)	95.74(11)
O(6)#2-Cd(2)-O(2)	150.28(9)	O(7)-Cd(2)-O(2)	84.12(10)
O(6)#2-Cd(2)-O(3)#4	87.83(10)	O(7)-Cd(2)-O(3)#4	82.33(11)
O(2)-Cd(2)-O(3)#4	121.42(10)	O(6)#2-Cd(2)-O(4)#4	113.97(11)
O(7)-Cd(2)-O(4)#4	124.81(11)	O(2)-Cd(2)-O(4)#4	89.54(10)
O(3)#4-Cd(2)-O(4)#4	55.31(10)	O(6)#2-Cd(2)-O(1)	95.12(9)
O(7)-Cd(2)-O(1)	81.83(9)	O(2)-Cd(2)-O(1)	55.34(8)
O(3)#4-Cd(2)-O(1)	164.09(10)	O(4)#4-Cd(2)-O(1)	135.52(9)
O(6)#2-Cd(2)-O(8)	75.63(9)	O(7)-Cd(2)-O(8)	152.40(9)
O(2)-Cd(2)-O(8)	90.79(9)	O(3)#4-Cd(2)-O(8)	122.70(10)
O(4)#4-Cd(2)-O(8)	82.11(9)	O(1)-Cd(2)-O(8)	73.09(8)

Symmetry transformations used to generate equivalent atoms:

#1 -x+1,-y+1,-z #2 x+1,y,z+1 #3 -x+2,-y+1,-z+1 #4 x,y+1,z+1

---

### Section 3. Detection of antibiotics



Scheme S2. Chemical structures of the antibiotics investigated.

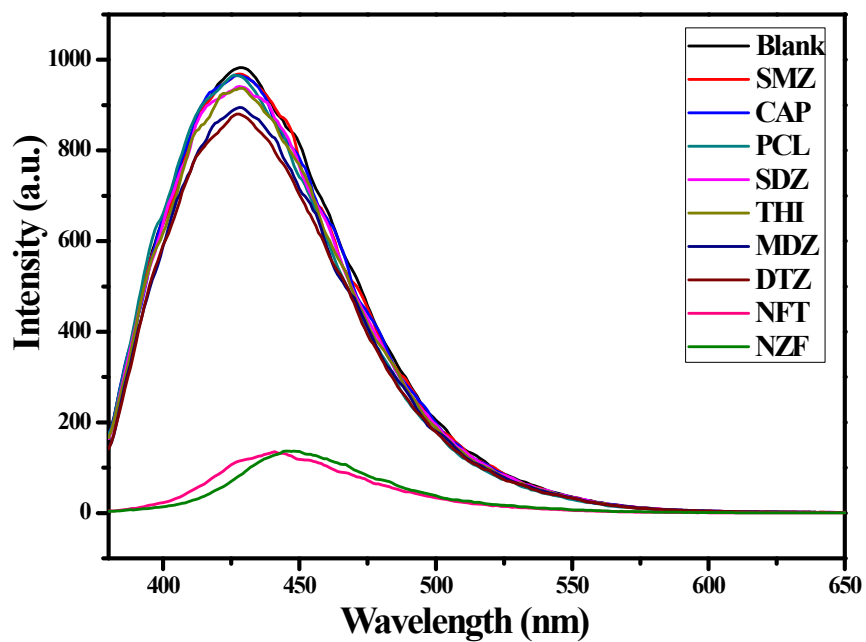
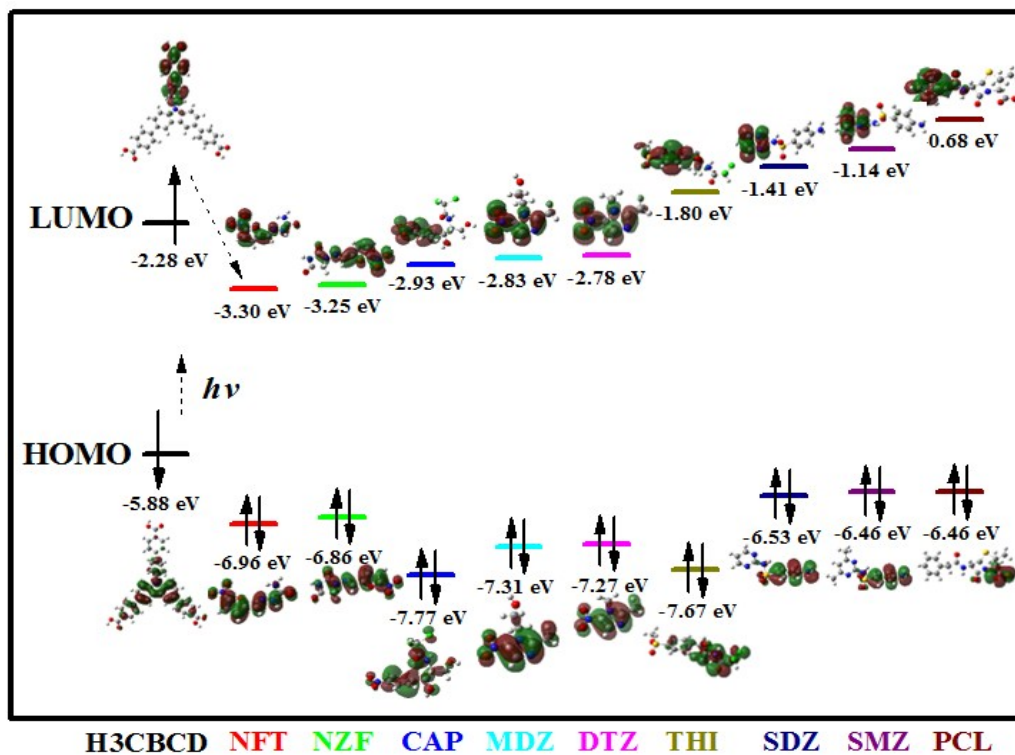
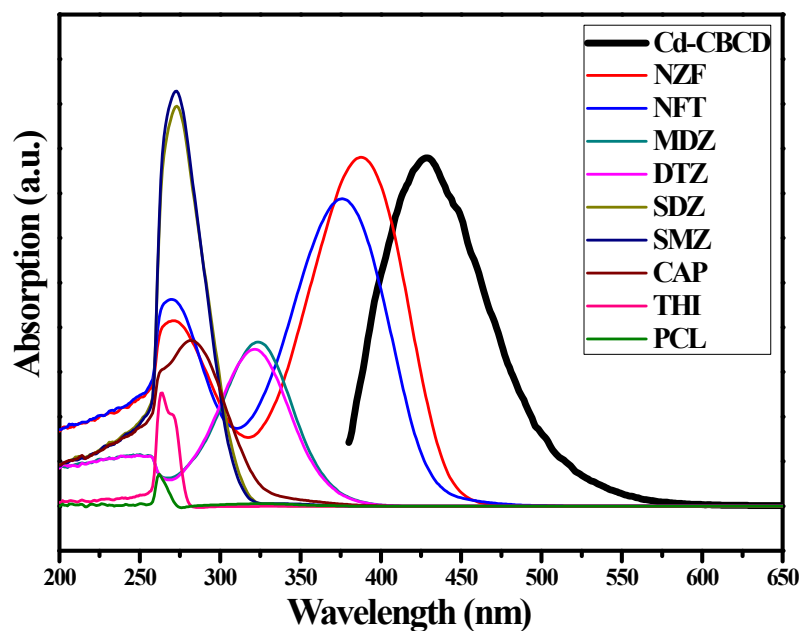


Fig. S10. Fluorescence spectra of Cd-CBCD dispersed in various 0.1 mM antibiotics.



**Fig. S11.** HOMO and LUMO energy levels of H<sub>3</sub>CBCD in Cd-CBCD and the selected antibiotics calculated by density functional theory (DFT) with B3LYP/6-31+G\* basis set.



**Fig. S12.** UV-vis absorption spectra of selected antibiotics (0.1 mM) and the normalized fluorescent emission spectra of Cd-CBCD in DMA.

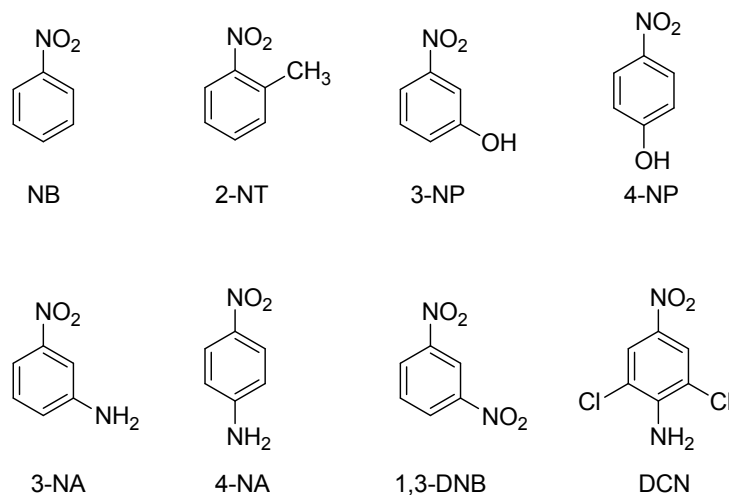
**Table S2.** Comparison of detection limits among other reported MOF materials and Cd-CBCD as the NZF/NFT sensor.

MOFs	Name	Analyte	$K_{sv}$ ( $M^{-1}$ )	Detection limits (ppb)	Ref.
Zr(IV)-Based MOFs	BUT-12	NZF	$1.1 \times 10^5$	58	1
	BUT-13	NZF	$7.5 \times 10^4$	90	
Cd(II)-Based MOFs	Sample 3	NZF	$5.06 \times 10^4$	162	2
		NFT	$3.57 \times 10^4$	274	
	Sample 4	NZF	$1.04 \times 10^5$	75	
		NFT	$7.19 \times 10^4$	131	
	Sample 5	NZF	$1.33 \times 10^5$	60	
NFT	$6.93 \times 10^4$	142			
In(III)-Based MOF	V102	NZF	$6.38 \times 10^4$	200	3
Zn(II)-Based MOF	Sample 1	NZF	---	100	4
Cd(II)-Based MOF	Cd-CBCD	NZF	$9.72 \times 10^4$	85	This work
		NFT	$6.39 \times 10^4$	128	

**Table S3.** HOMO and LUMO energies for the selected antibiotics calculated by density functional theory (DFT) with B3LYP/6-31+G\* basis set.

<b>Analytes</b>	<b>HUMO (eV)</b>	<b>LUMO (eV)</b>	<b>Band Gap (eV)</b>
PCL	-6.46285	-0.67812	5.78473
SMZ	-6.46258	-1.13773	5.32485
SDZ	-6.52544	-1.40958	5.11586
THI	-7.66671	-1.79735	5.86936
DTZ	-7.26914	-2.78052	4.48862
MDZ	-7.30669	-2.83495	4.47174
CAP	-7.76821	-2.92992	4.83829
NZF	-6.85634	-3.24612	3.61022
NFT	-6.95838	-3.30218	3.6562

## Section 4. Detection of NACs and pesticides



**Scheme S3.** Chemical structures of NACs and DCN.

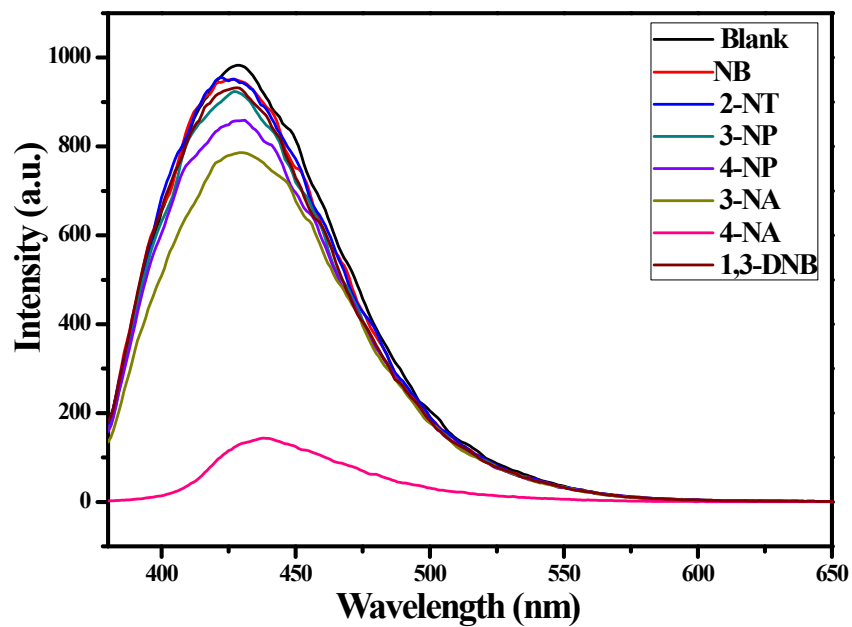


**Fig. S13.** Fluorescence spectra of Cd-CBCD dispersed in various 0.1 mM NACs.

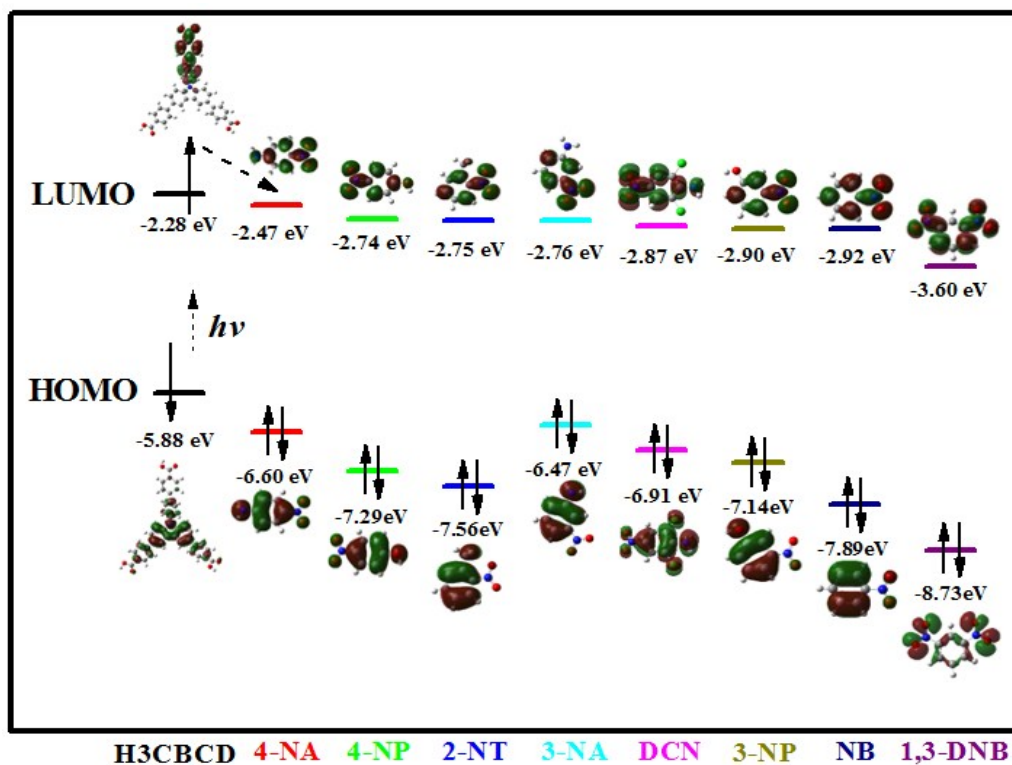


**Fig. S14.** HOMO and LUMO energy levels of H<sub>3</sub>CBCD in Cd-CBCD and the selected NACs and DCN calculated by density functional theory (DFT) with B3LYP/6-31+G\* basis set.

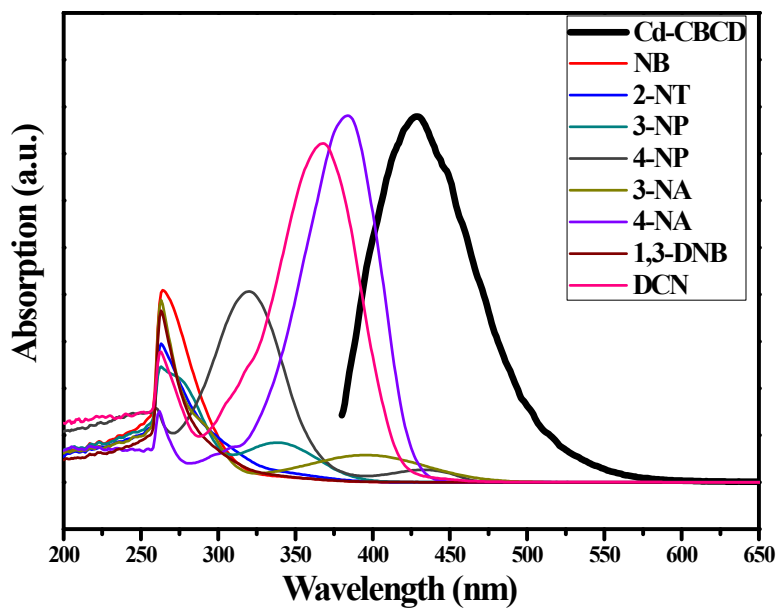


**Fig. S15.** UV-vis absorption spectra of selected NACs and DCN (0.1 mM) and the normalized fluorescent emission spectra of Cd-CBCD in DMA.



**Table S4.** Performance comparison between various MOF fluorescent sensors for the detection of 4-NA.

LMOFs	$K_{sv}$ ( $M^{-1}$ )	Detection limits (ppb)	Ref.
$\{Cd(ppvppa)(1,4-NDC)\}_n$	13	$1.2 \times 10^5$	5
$Zn_3L_3(DMA)_2(H_2O)_3$	$2.18 \times 10^4$	---	6
Cd-PDA	$4.08 \times 10^4$	3.5	7
$\{[Cd(5-asba)-(bimb)]\}_n$	$9.80 \times 10^4$	520	8
$[Cd_3(DBPT)_2(H_2O)_4] \cdot 5H_2O$	$2.50 \times 10^4$	700	9
Cd-CBCD	$5.70 \times 10^4$	116	This work

**Table S5.** HOMO and LUMO energies for the selected NACs and DCN calculated by density functional theory (DFT) with B3LYP/6-31+G\* basis set.

Analytes	HUMO (eV)	LUMO (eV)	Band Gap (eV)
NB	-7.88849	-2.91549	4.97299
2-NT	-7.55514	-2.74814	4.80700
3-NP	-7.13961	-2.90352	4.23609
4-NP	-7.29064	-2.74079	4.54985
3-NA	-6.47210	-2.75630	3.71580
4-NA	-6.59673	-2.47303	4.12370
1,3-DNB	-8.73179	-3.59797	5.13382
DCN	-6.90994	-2.86570	4.04424

## References

1. B. Wang, X.-L. Lv, D. Feng, L.-H. Xie, J. Zhang, M. Li, Y. Xie, J.-R. Li and H.-C. Zhou, *J. Am. Chem. Soc.*, 2016, **138**, 6204-6216.
2. D. Zhao, X.-H. Liu, Y. Zhao, P. Wang, Y. Liu, M. Azam, S. I. Al-Resayes, Y. Lu and W.-Y. Sun, *J. Mater. Chem. A*, 2017, **5**, 15797-15807.
3. S.-L. Hou, J. Dong, X.-L. Jiang, Z.-H. Jiao, C.-M. Wang and B. Zhao, *Anal. Chem.*, 2018, **90**, 1516-1519.
4. X.-G. Liu, C.-L. Tao, H.-Q. Yu, B. Chen, Z. Liu, G.-P. Zhu, Z. Zhao, L. Shen and B. Z. Tang, *J. Mater. Chem. C*, 2018, **6**, 2983-2988.
5. M. M. Chen, X. Zhou, H. X. Li, X. X. Yang and J. P. Lang, *Cryst. Growth Des.*, 2015, **15**, 2753-2760.
6. Z. C. Yu, F. Q. Wang, X. Y. Lin, C. M. Wang, Y. Y. Fu, X. J. Wang, Y. N. Zhao and G. D. Li, *J. Solid State Chem.*, 2015, **232**, 96-101.
7. P. Y. Wu, Y. H. Liu, Y. Li, M. Jiang, X. L. Li, Y. H. Shi and J. Wang, *J. Mater. Chem. A*, 2016, **4**, 16349-16355.
8. Y. J. Yang, M. J. Wang and K. L. Zhang, *J. Mater. Chem. C*, 2016, **4**, 11404-11418.
9. B. X. Dong, Y. M. Pan, W. L. Liu and Y. L. Teng, *Cryst. Growth Des.*, 2018, **18**, 431-440.